KANAZAWA-12-07

Multi-Component Dark Matter Systems and Their Observation Prospects

Mayumi Aoki,[1,2,*] Michael Duerr,[2,†] Jisuke Kubo,[1,‡] and Hiroshi Takano[1,§]

[1] *Institute for Theoretical Physics, Kanazawa University, Kanazawa 920-1192, Japan*

[2] *Max–Planck–Institut für Kernphysik, Saupfercheckweg 1, 69117 Heidelberg, Germany*

Abstract

Conversions and semi-annihilations of dark matter (DM) particles in addition to the standard DM annihilations are considered in a three-component DM system. We find that the relic abundance of DM can be very sensitive to these non-standard DM annihilation processes, which has been recently found for two-component DM systems. To consider a concrete model of a three-component DM system, we extend the radiative seesaw model of Ma by adding a Majorana fermion χ and a real scalar boson ϕ, to obtain a $Z_2 \times Z_2'$ DM stabilizing symmetry, where we assume that the DM particles are the inert Higgs boson, χ and ϕ. It is shown how the allowed parameter space, obtained previously in the absence of χ and ϕ, changes. The semi-annihilation process in this model produces monochromatic neutrinos. The observation rate of these monochromatic neutrinos from the Sun at IceCube is estimated. Observations of high energy monochromatic neutrinos from the Sun may indicate a multi-component DM system.

PACS numbers: 95.35.+d, 95.85.Ry, 11.30.Er

*Electronic address: mayumi@hep.s.kanazawa-u.ac.jp

†Electronic address: michael.duerr@mpi-hd.mpg.de

‡Electronic address: jik@hep.s.kanazawa-u.ac.jp

§Electronic address: takano@hep.s.kanazawa-u.ac.jp

I. INTRODUCTION

Recent astrophysical observations [1–3] have made it clear that most of the energy of the universe consists of dark energy and cold dark matter (DM), and their portions are very well fixed by these observations. While the origin of dark energy might be the cosmological constant of Einstein, the origin of cold DM cannot be found within the framework of the standard model (SM) of elementary particles. Moreover, we do not know very much about the detailed features of DM at present, even if the origin of DM should be elementary particles. Currently, many experiments are undertaken or planned, and it is widely believed that the existence of DM will be independently confirmed in the near future (see, for instance, [4–6]).

A particle DM candidate can be made stable by an unbroken symmetry. The simplest possibility of such a symmetry is a parity, Z_2. Whatever the origin of the Z_2 is, the lightest Z_2 odd particle can be a DM candidate if it is a neutral, weakly interacting and massive particle (WIMP) (see [5] for a review). There is a variety of origins of the Z_2. R parity in the minimal supersymmetric standard model (MSSM), which is introduced to forbid fast proton decay, is a well-known example (see [4] for a review). In this paper we consider a universe consisting of stable multi DM particles [7]–[28]. A multi-component DM system can be realized if the DM stabilizing symmetry is larger than Z_2: Z_N ($N \geq 4$) or a product of two or more Z_2's can yield a multi-component DM system.[1] In a supersymmetric extension of the radiative seesaw model of [31], for instance, a $Z_2 \times Z_2'$ symmetry appears, providing various concrete models of multi-component DM systems [24]–[28].

In a multi-component DM system, there can be various DM annihilation processes that are different from the standard DM annihilation process [32]–[37], DM DM $\to XX$, where X is a generic SM particle in thermal equilibrium. Even in one-component DM systems, the non-standard annihilation process, the co-annihilation of DM and a nearly degenerate unstable particle [38], can play a crucial role in the MSSM [39]. The importance of non-standard annihilation processes such as DM conversion [16, 21, 22] and semi-annihilation of DM [16, 22] in two-component DM systems for the temperature evolution of the number density of DM has been recently reported.

If $(Z_2)^\ell$ is unbroken, there can exist at least $K = \ell$ stable DM particles. In a kinematically fortunate situation, $2^\ell - 1$ stable DM particles can exist; for $\ell = 2$ there can be maximally $K = 3$ stable DM particles. Any one-component DM model can easily be extended to a multi-component DM system. The allowed parameter space of a one-component DM model can considerably change, as it has been recently found in [28] (see also [9]), even using a crude approximation of a DM conversion process in a supersymmetric extension of the radiative seesaw model.

In Sect. II, after we will have outlined a derivation of the coupled Boltzmann equations

[1] Z_3 allows only one-component DM systems. Refs. [29, 30] discuss models with Z_3.

that are appropriate for our purpose, we will consider fictive two- and three-component DM systems and analyze the effects of non-standard annihilation processes of DM. We will also address the question, within the framework of thermally produced DM [32], whether one can obtain a large boost factor in a three-component DM system that is needed to explain [40] the positron excess observed by recent experiments [41]–[44]. We will find that in a fortunate situation a boost factor of $O(10)$ can be obtained, which can be combined with the known mechanisms [45]–[50], to obtain a desired enhancement effect.

In Sect. III we will extend the radiative seesaw model of [31] by adding an extra Majorana fermion χ and an extra real scalar boson ϕ so as to obtain $Z_2 \times Z_2'$ as a DM stabilizing symmetry. Apart from the presence of ϕ, the Higgs sector is identical to that of [51–53]. This model shall show how the allowed parameter space, which is obtained in [51–53] under the assumption that the lightest inert Higgs boson is DM, can change. Indirect detection of DM, in particular of neutrinos from the annihilation of the captured DM in the Sun [54]–[63] are also discussed. We will solve the coupled evolution equations of the DM numbers in the Sun, which describe approaching equilibrium between the capture and annihilation (including conversion and semi-annihilation) rates of DM, and estimate the observation rates of neutrinos. Due to semi-annihilations of DM, monochromatic neutrinos are radiated from the Sun. Our conclusions are given in Sect. IV.

II. BOLTZMANN EQUATION AND TWO- AND THREE-COMPONENT DM SYSTEMS

A. Boltzmann equation

Here we would like to outline a derivation of the Boltzmann equation that we are going to apply in the next section. We will do it for completeness, although the following discussion partially parallels that of [16] (see also [21]). We start by assuming the existence of K stable DM particles χ_i with mass m_i. None of the DM particles have the same quantum number with respect to the DM stabilizing symmetry. All the other particles are supposed to be in thermal equilibrium. Then we restrict ourselves to three types of processes which enter the Boltzmann equation:

$$\chi_i\ \chi_i \leftrightarrow X_i\ X_i' \ , \tag{1}$$

$$\chi_i\ \chi_i \leftrightarrow \chi_j\ \chi_j \ \text{(DM conversion)} \ , \tag{2}$$

$$\chi_i\ \chi_j \leftrightarrow \chi_k\ X_{ijk} \ \text{(DM semi-annihilation)} \ , \tag{3}$$

where the extension to include coannihilations and annihilation processes like $\chi_i + \chi_j \leftrightarrow \chi_k + \chi_l$ is straight forward. See Fig. 1 for a depiction of DM conversion and DM semi-annihilation. We denote the phase space density of χ_i by $f_i(E_i, t)$ and its number density by $n_i(t) = (g/(2\pi)^3) \int d^3p_i f_i(E_i, t)$, where g stands for the internal degrees of freedom. Then

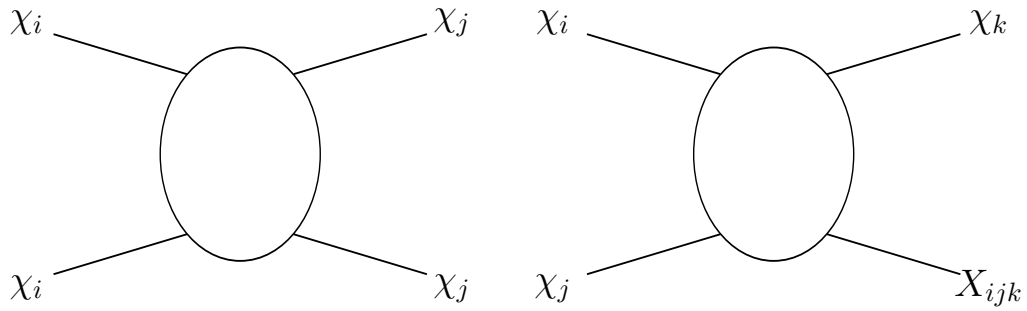

FIG. 1: Dark matter conversion (left) and semi-annihilation (right).

the density n_i satisfies the Boltzmann equation (see, e.g., [35]), which we will not spell out here. Instead, we make the replacement

$$t \;=\; 0.301 g_*^{-1/2} M_{\rm PL} T^{-2} \tag{4}$$

during the radiation-dominated epoch, where t is the time of the comoving frame, g_* is the total number of effective degrees of freedom, T and $M_{\rm PL}$ are the temperature and the Planck mass, respectively. Further, we use the approximation

$$\frac{f_i(E_i,t)}{\bar{f}_i(E_i,t)} \;\simeq\; \frac{n_i(t)}{\bar{n}_i(t)} \;, \tag{5}$$

where $\bar{f}_i(E_i,t) \simeq \exp(-E_i/T)$ and $\bar{n}_i = (g/(2\pi)^3)\int d^3p_i \bar{f}_i(E_i,t)$ are the values in equilibrium, and we ignore the chemical potential. Then the collision terms in the Boltzmann equation can be written as

$$\begin{aligned}
&-(\mathrm{PSI})|M(ii;X_iX_i')|^2 \frac{\bar{f}_i\bar{f}_i}{\bar{n}_i\bar{n}_i}\,(n_in_i-\bar{n}_i\bar{n}_i) \\
&-\sum_{i>j}(\mathrm{PSI})\;|M(ii;jj)|^2 \frac{\bar{f}_i\bar{f}_i}{\bar{n}_i\bar{n}_i}\left(n_in_i-\frac{n_jn_j}{\bar{n}_j\bar{n}_j}\bar{n}_i\bar{n}_i\right) \\
&+\sum_{j>i}(\mathrm{PSI})\;|M(jj;ii)|^2 \frac{\bar{f}_j\bar{f}_j}{\bar{n}_j\bar{n}_j}\left(n_jn_j-\frac{n_in_i}{\bar{n}_i\bar{n}_i}\bar{n}_j\bar{n}_j\right) \\
&-\sum_{j,k}(\mathrm{PSI})\;|M(ij;kX_{ijk})|^2 \frac{\bar{f}_i\bar{f}_j}{\bar{n}_i\bar{n}_j}\left(n_in_j-\frac{n_k}{\bar{n}_k}\bar{n}_i\bar{n}_j\right) \\
&+\sum_{j,k}(\mathrm{PSI})\;|M(jk;iX_{jki})|^2 \frac{\bar{f}_j\bar{f}_k}{\bar{n}_j\bar{n}_k}\left(n_jn_k-\frac{n_i}{\bar{n}_i}\bar{n}_j\bar{n}_k\right) \;,
\end{aligned} \tag{6}$$

where PSI stands for "phase space integral of $(2\pi)^4\delta^4(\mathrm{momenta})\times$", M is the matrix element of the corresponding process, and we have assumed that

$$m_i \;\geq\; m_j \text{ for } i>j \;\text{ and }\; m_{X_i}, m_{X_i'}, m_{X_{ijk}} << m_l \text{ for all } i,j,k,l \;. \tag{7}$$

Using the notion of the thermally-averaged cross section,

$$< \sigma(ii; X_i X_i')v > \; = \; \frac{1}{\bar{n}_i \bar{n}_i} \mathrm{PSI} |M(ii; X_i X_i')|^2 \bar{f}_i \bar{f}_i \; , \tag{8}$$

and the dimensionless inverse temperature $x = \mu/T$, we obtain for the number per comoving volume $Y_i = n_i/s$:

$$\begin{aligned}
\frac{dY_i}{dx} = & -0.264 \; g_*^{1/2} \left[\frac{\mu M_{\mathrm{PL}}}{x^2} \right] \Big\{ \; < \sigma(ii; X_i X_i')v > \left(Y_i Y_i - \bar{Y}_i \bar{Y}_i \right) \\
& + \sum_{i>j} < \sigma(ii; jj)v > \left(Y_i Y_i - \frac{Y_j Y_j}{\bar{Y}_j \bar{Y}_j} \bar{Y}_i \bar{Y}_i \right) - \sum_{j>i} < \sigma(jj; ii)v > \left(Y_j Y_j - \frac{Y_i Y_i}{\bar{Y}_i \bar{Y}_i} \bar{Y}_j \bar{Y}_j \right) \\
& + \sum_{j,k} < \sigma(ij; k X_{ijk})v > \left(Y_i Y_j - \frac{Y_k}{\bar{Y}_k} \bar{Y}_i \bar{Y}_j \right) - \sum_{j,k} < \sigma(jk; i X_{jki})v > \left(Y_j Y_k - \frac{Y_i}{\bar{Y}_i} \bar{Y}_j \bar{Y}_k \right) \Big\} \; ,
\end{aligned} \tag{9}$$

where $1/\mu = (\sum_i m_i^{-1})$ is the reduced mass of the system. To arrive at Eq. (9) we have used: $s = (2\pi^2/45) g_* T^3$, $H = 1.66 \times g_*^{1/2} T^2 / M_{\mathrm{PL}}$, where s is the entropy density, and H is the Hubble constant.

We will integrate this system of coupled non-linear differential equations numerically. Before we apply the Boltzmann equation (9) to a concrete DM model, we discuss below the cases of $K = 2$ and 3 simply assuming fictitious values of the thermally-averaged cross sections and DM masses m_i.

B. Two-component DM system

Before we come to one of our main interests, a three-component DM system, we first consider the $K = 2$ case with a $Z_2 \times Z_2'$ symmetry. In this case, there are three different thermally-averaged cross sections. No semi-annihilation (3) is allowed due to $Z_2 \times Z_2'$.[2] We further assume that there are only s-wave contributions to $< \sigma v >$ and X_i $(i = 1, 2)$ are massless while $m_1 \geq m_2$:

$$\begin{aligned}
< \sigma(11; X_1 X_1')v > \; &= \; \sigma_{0,1} \times 10^{-9} \; \mathrm{GeV}^{-2} \; , \quad < \sigma(22; X_2 X_2')v > = \sigma_{0,2} \times 10^{-9} \; \mathrm{GeV}^{-2} \; , \\
< \sigma(11; 22)v > \; &= \; \sigma_{0,12} \times 10^{-9} \; \mathrm{GeV}^{-2} \; .
\end{aligned} \tag{10}$$

Eq. (9) then becomes

$$\begin{aligned}
\frac{dY_1}{dx} = & -0.264 \; g_*^{1/2} \left[\frac{\mu M_{\mathrm{PL}}}{x^2} \right] \Big\{ < \sigma(11; X_1 X_1')v > \left(Y_1 Y_1 - \bar{Y}_1 \bar{Y}_1 \right) \\
& + < \sigma(11; 22)v > \left(Y_1 Y_1 - \frac{Y_2 Y_2}{\bar{Y}_2 \bar{Y}_2} \bar{Y}_1 \bar{Y}_1 \right) \Big\} \; ,
\end{aligned} \tag{11}$$

[2] In Refs. [16, 22], the Z_4 case is discussed in detail. In this case there exist two independent DM particles, because due to CP invariance the anti-particle is not an independent degree of freedom in the Boltzmann equation. Semi-annihilation is allowed in this case.

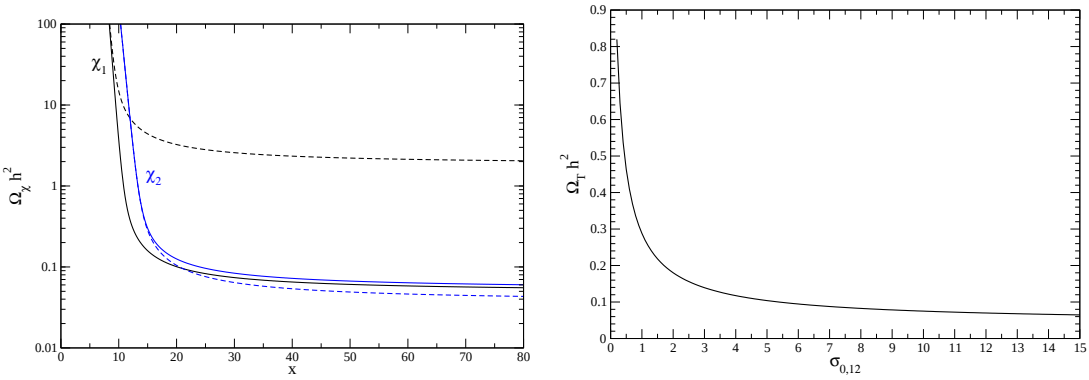

FIG. 2: Left: The relic abundance $\Omega_{\chi_1}h^2(x)$ (black) and $\Omega_{\chi_2}h^2(x)$ (blue) as a function of $x = \mu/T = [(m_1^{-1} + m_2^{-1})T]^{-1}$ with $\sigma_{0,1} = 0.1$, $\sigma_{0,2} = 6$, $\sigma_{0,12} = 4.4(0)$ (solid (dashed)) , $m_1 = 200$ GeV, $m_2 = 160$ GeV and $g_* = 90$. Right: The total relic abundance $\Omega_T h^2$ as a function of $\sigma_{0,12}$ which parametrizes the size of the conversion $\chi_1\chi_1 \to \chi_2\chi_2$.

$$\frac{dY_2}{dx} = -0.264\ g_*^{1/2}\left[\frac{\mu M_{\rm PL}}{x^2}\right]\Big\{<\sigma(22; X_2X_2')v>\left(Y_2Y_2 - \bar{Y}_2\bar{Y}_2\right) - <\sigma(11;22)v>\left(Y_1Y_1 - \frac{Y_2Y_2}{\bar{Y}_2\bar{Y}_2}\bar{Y}_1\bar{Y}_1\right)\Big\}\ . \tag{12}$$

We consider the case in which the size of the DM conversion and the standard annihilation are of similar order (see also [21]). In Fig. 2 (left) we show the evolution of the fraction of critical densities, $\Omega_{\chi_1}h^2(x)$ (black) and $\Omega_{\chi_2}h^2(x)$ (blue), contributed by χ_1 and χ_2, respectively, where we have used $\sigma_{0,1} = 0.1$, $\sigma_{0,2} = 6$, $\sigma_{0,12} = 4.4(0)$ (solid (dashed)) , $m_1 = 200$ GeV, $m_2 = 160$ GeV and $g_* = 90$, and $x = \mu/T = [(m_1^{-1} + m_2^{-1})T]^{-1}$. As we see from Fig. 2 (left), at $\sigma_{0,12} = 0$ (i.e., no DM conversion (2)), the density of χ_1 decouples from the equilibrium value for smaller x than the density of χ_2. This is because we have chosen a small value for $\sigma_{0,1}$ and a large value for $\sigma_{0,2}$. At $\sigma_{0,12} = 0$, $\Omega_{\chi_1}h^2 \approx 1.99$, while $\Omega_{\chi_2}h^2 \approx 0.04$. With increasing value of $\sigma_{0,12}$ (which parametrizes the size of the DM conversion (2)), $\Omega_{\chi_1}h^2$ decreases, while $\Omega_{\chi_2}h^2$ increases. Around $\sigma_{0,12} = 3.9$, this order changes, i.e., $\Omega_{\chi_1} < \Omega_{\chi_2}$. At $\sigma_{0,12} = 4.4$, we obtain the total relic abundance $\Omega_T h^2 = \Omega_{\chi_1}h^2 + \Omega_{\chi_2}h^2 = 0.112$, in accord with the WMAP observation $\Omega_T h^2 = 0.1126 \pm 0.0036$ [3]. In Fig. 2 (right) we plot $\Omega_T h^2$ as a function of $\sigma_{0,12}$. We see that the DM conversion process plays an important role, as it has been also found in [11, 16, 21, 22].

C. Three-component DM system

As we have noticed before, the $K = 3$ case is possible even for a $Z_2 \times Z_2'$ symmetry if the decay of χ_i is kinematically forbidden. In this case there are nine different thermally-averaged cross sections, if we assume that $m_1 \geq m_2 \geq m_3$ and $m_2 + m_3 > m_1$:

$$<\sigma(ii; X_iX_i')v> \ = \ \sigma_{0,i} \times 10^{-9}\ \text{GeV}^{-2}\ , \quad <\sigma(11;22)v> = \sigma_{0,12} \times 10^{-9}\ \text{GeV}^{-2}\ ,$$

$$
\begin{aligned}
<\sigma(11;33)v> &= \sigma_{0,13}\times 10^{-9}\ \text{GeV}^{-2}\ , \quad <\sigma(22;33)v>=\sigma_{0,23}\times 10^{-9}\ \text{GeV}^{-2}\ , \\
<\sigma(12;3X_{123})v> &= \sigma_{0,123}\times 10^{-9}\ \text{GeV}^{-2}\ , \quad <\sigma(23;1X_{231})v>=\sigma_{0,231}\times 10^{-9}\ \text{GeV}^{-2}\ , \\
<\sigma(31;2X_{312})v> &= \sigma_{0,312}\times 10^{-9}\ \text{GeV}^{-2}\ . \qquad (13)
\end{aligned}
$$

Eq. (9) then becomes

$$
\begin{aligned}
\frac{dY_1}{dx} &= -0.264\ g_*^{1/2}\left[\frac{\mu M_{\rm PL}}{x^2}\right]\Big\{<\sigma(11;X_1X_1')v>\left(Y_1Y_1-\bar{Y}_1\bar{Y}_1\right) \\
&+<\sigma(11;22)v>\left(Y_1Y_1-\frac{Y_2Y_2}{\bar{Y}_2\bar{Y}_2}\bar{Y}_1\bar{Y}_1\right)+<\sigma(11;33)v>\left(Y_1Y_1-\frac{Y_3Y_3}{\bar{Y}_3\bar{Y}_3}\bar{Y}_1\bar{Y}_1\right) \\
&+<\sigma(12;3X_{123})v>\left(Y_1Y_2-\frac{Y_3}{\bar{Y}_3}\bar{Y}_1\bar{Y}_2\right)+<\sigma(31;2X_{312})v>\left(Y_1Y_3-\frac{Y_2}{\bar{Y}_2}\bar{Y}_1\bar{Y}_3\right) \\
&-<\sigma(23;1X_{231})v>\left(Y_3Y_2-\frac{Y_1}{\bar{Y}_1}\bar{Y}_3\bar{Y}_2\right)\Big\}\ , \qquad (14) \\
\frac{dY_2}{dx} &= -0.264\ g_*^{1/2}\left[\frac{\mu M_{\rm PL}}{x^2}\right]\Big\{<\sigma(22;X_2X_2')v>\left(Y_2Y_2-\bar{Y}_2\bar{Y}_2\right) \\
&+<\sigma(22;33)v>\left(Y_2Y_2-\frac{Y_3Y_3}{\bar{Y}_3\bar{Y}_3}\bar{Y}_2\bar{Y}_2\right)+<\sigma(23;1X_{231})v>\left(Y_2Y_3-\frac{Y_1}{\bar{Y}_1}\bar{Y}_2\bar{Y}_3\right) \\
&+<\sigma(12;3X_{123})v>\left(Y_1Y_2-\frac{Y_3}{\bar{Y}_3}\bar{Y}_1\bar{Y}_2\right)-<\sigma(31;2X_{312})v>\left(Y_1Y_3-\frac{Y_2}{\bar{Y}_2}\bar{Y}_1\bar{Y}_3\right) \\
&-<\sigma(11;22)v>\left(Y_1Y_1-\frac{Y_2Y_2}{\bar{Y}_2\bar{Y}_2}\bar{Y}_1\bar{Y}_1\right)\Big\}\ , \qquad (15) \\
\frac{dY_3}{dx} &= -0.264\ g_*^{1/2}\left[\frac{\mu M_{\rm PL}}{x^2}\right]\Big\{<\sigma(33;X_3X_3')v>\left(Y_3Y_3-\bar{Y}_3\bar{Y}_3\right) \\
&+<\sigma(23;1X_{231})v>\left(Y_2Y_3-\frac{Y_1}{\bar{Y}_1}\bar{Y}_2\bar{Y}_3\right)+<\sigma(31;2X_{312})v>\left(Y_1Y_3-\frac{Y_2}{\bar{Y}_2}\bar{Y}_1\bar{Y}_3\right) \\
&-<\sigma(12;3X_{123})v>\left(Y_1Y_2-\frac{Y_3}{\bar{Y}_3}\bar{Y}_1\bar{Y}_2\right)-<\sigma(11;33)v>\left(Y_1Y_1-\frac{Y_3Y_3}{\bar{Y}_3\bar{Y}_3}\bar{Y}_1\bar{Y}_1\right) \\
&-<\sigma(22;33)v>\left(Y_2Y_2-\frac{Y_3Y_3}{\bar{Y}_3\bar{Y}_3}\bar{Y}_2\bar{Y}_2\right)\Big\}\ , \qquad (16)
\end{aligned}
$$

where $1/\mu = 1/m_1 + 1/m_2 + 1/m_3$.

As a representative example we consider the following set of input values of the parameters:

$$
\begin{aligned}
m_1 &= 200\ \text{GeV}\ ,\ m_2 = 160\ \text{GeV}\ ,\ m_3 = 140\ \text{GeV}\ , \\
\sigma_{0,1} &= 0.1\ ,\ \sigma_{0,2} = 2\ ,\ \sigma_{0,3} = 6\ . \qquad (17)
\end{aligned}
$$

First we show the evolution of $\Omega_{\chi_i}h^2(x)$ in Fig. 3 (left) for $\sigma_{0,12} = \sigma_{0,13} = \sigma_{0,23} = \sigma_{0,123} = \sigma_{0,312} = \sigma_{0,231} = 0$, which corresponds to the situation without the non-standard annihilation processes. Since $m_1 > m_2, m_3$ and the cross section $\sigma(11; X_1X_1)$ is small in this example, the relic abundance of χ_1 is large compared with that of χ_2 and χ_3. This changes if we switch on the non-standard annihilation processes. This is shown in Fig. 3 (right), where we have used $\sigma_{0,12} = \sigma_{0,13} = \sigma_{0,23} = 5.2$, while $\sigma_{0,123} = \sigma_{0,312} = \sigma_{0,231} = 0$ to see the effects

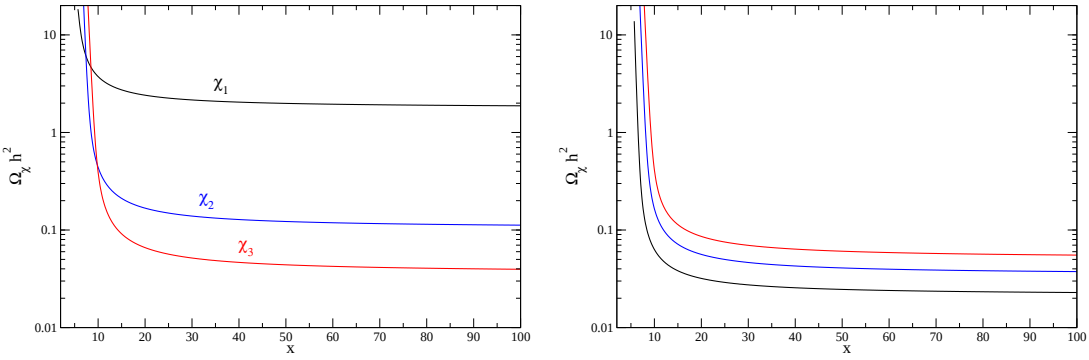

FIG. 3: The relic abundance $\Omega_{\chi_1}h^2(x)$ (black), $\Omega_{\chi_2}h^2(x)$ (blue) and $\Omega_{\chi_3}h^2(x)$ (red) as a function of $x = \mu/T = [(m_1^{-1} + m_2^{-1} + m_3^{-1})T]^{-1}$, where the input parameters are given in Eq. (17). Left: Without the non-standard annihilation processes (2) and (3). Right: $\sigma_{0,12} = \sigma_{0,13} = \sigma_{0,23} = 5.2$, while $\sigma_{0,123} = \sigma_{0,312} = \sigma_{0,231} = 0$ to see the effects of $\chi_i\chi_i \leftrightarrow \chi_j\chi_j$ type processes (3).

of $\chi_i\chi_i \leftrightarrow \chi_j\chi_j$ type processes (DM conversion). As expected, the relic abundances of χ_1 and χ_2 decrease and drop below 0.1, while that of χ_3 does not change very much.

Fig. 4 shows the evolution of $\Omega_{\chi_i}h^2(x)$ for $\sigma_{0,12} = \sigma_{0,13} = \sigma_{0,23} = 0$, while $\sigma_{0,123} = \sigma_{0,312} = \sigma_{0,231} = 5.1$ to see the effects of $\chi_i\chi_j \leftrightarrow \chi_k X_{ijk}$ type processes (semi-annihilation). It is interesting to observe that the order of the relic abundances changes and $\Omega_{\chi_1}h^2(x)$ first decreases as usual, but then starts to increase towards the freeze-out value. So, the effects of $\chi_i\chi_i \leftrightarrow \chi_j\chi_j$ type and $\chi_i\chi_j \leftrightarrow \chi_k X_{ijk}$ type processes are different. In the examples above, $\sigma_{0,ij}$ and $\sigma_{0,ijk}$ are chosen such that the total abundance $\Omega_T h^2$ becomes about the realistic value 0.112. In Fig. 5 we show the total abundance $\Omega_T h^2$ as a function of $\sigma_{0,ij}$ (solid) and $\sigma_{0,ijk}$ (dashed), where $\sigma_{0,ij}$ parameterizes the size of the DM conversion (2) and $\sigma_{0,ijk}$ parameterizes the size of the semi-annihilation (3). As we can see from Fig. 5, only for small values of $\sigma_{0,ij}$ and $\sigma_{0,ijk}$ the effects on $\Omega_T h^2$ are different.

Next we would like to address the question whether one can obtain a boost factor in the case of $K = 3$ within the framework of thermally produced DM,[3] where as before we assume that $m_1 \geq m_2 \geq m_3$ and $m_2 + m_3 > m_1$. Here we are interested in the situation that the scales that enter into the Boltzmann equations (9) are not extremely different, because this situation can easily be realized in many phenomenologically viable models. The parameter space for the case $K = 3$ is large, and therefore, to simplify the situation, we assume that only semi-annihilations (3) are present. We further assume that all the semi-annihilation processes (3) produce the same SM model particle X, whose mass can be neglected. Then the differential energy flux Φ_X of X produced from the DM semi-annihilations can be written

[3] Non-standard freeze-out history of DM in the $K = 2$ component DM system has been considered in [13, 19] and a large boost factor of $O(1000)$ has been found.

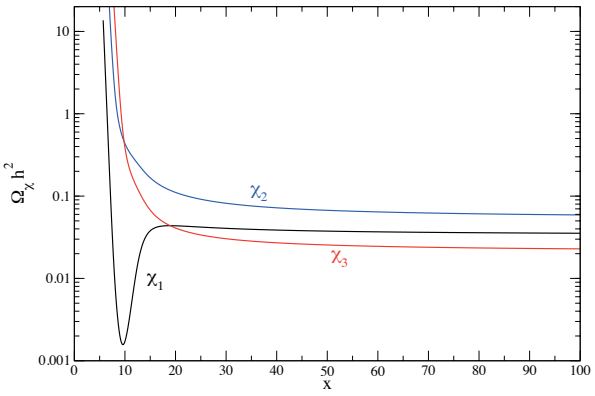

FIG. 4: The relic abundance $\Omega_{\chi_1}h^2(x)$ (black), $\Omega_{\chi_2}h^2(x)$ (blue) and $\Omega_{\chi_3}h^2(x)$ (red) as a function of x with $\sigma_{0,12} = \sigma_{0,13} = \sigma_{0,23} = 0$, while $\sigma_{0,123} = \sigma_{0,312} = \sigma_{0,231} = 5.1$ to see the effects of $\chi_i\chi_j \leftrightarrow \chi_k X_{ijk}$ type processes (3).

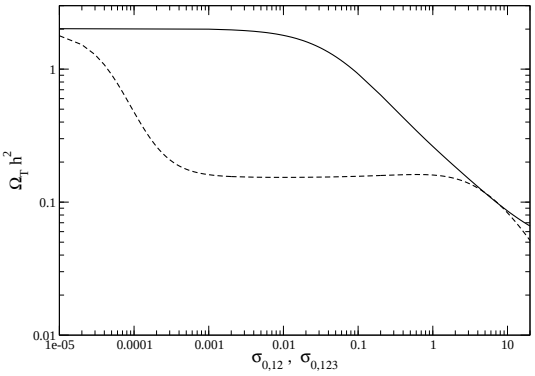

FIG. 5: The total relic abundance $\Omega_T h^2$ as a function of $\sigma_{0,12}$ (solid) and $\sigma_{0,123}$ (dashed). Except $\sigma_{0,12}$ (DM conversion) and $\sigma_{0,123}$ (semi-annihilation) the input parameters are given in Eq. (17).

as

$$\frac{d\Phi_X}{dE_X} \propto \sum_{i<j} N_X^{ij}\, n_{i,\infty} n_{j,\infty} \; < \sigma(ij;kX)v > \;\; , \tag{18}$$

where $n_{i,\infty}$ is the freeze-out value of n_i, and N_X^{ij} and E_X stand for the number and the energy of X in the process $\chi_i\chi_j \to \chi_k X$, respectively. Eq. (18) suggests the following definition of the effective boost factor:

$$BF_X \;=\; \frac{\sum_{i<j} Y_{i,\infty} Y_{j,\infty} < \sigma(ij;kX)v >}{Y^0_{2,\infty} Y^0_{2,\infty} < \sigma(22;X)v >^0} \;\; , \tag{19}$$

where $Y_{i,\infty}$ is the freeze-out value of Y_i. The quantities with the superscript 0 in the denominator are the reference quantities. Here we use as reference the one-component DM case with only the standard annihilation process $\chi_2\chi_2 \to XX$, which means $Y^0_{2,\infty} \simeq$

TABLE I: The effective boost factor BF_X (19) for the symmetric case, i.e., $\sigma_{0,123} = \sigma_{0,231} = \sigma_{0,312}$, with $m_1 = 1000$ GeV.

m_2	m_3	$\sigma_{0,123}$	$\Omega_{\chi_1}h^2$	$\Omega_{\chi_2}h^2$	$\Omega_{\chi_3}h^2$	BF_X
720	700	12.6	0.0433	0.0319	0.0372	1.6
940	700	417.0	0.0007	0.0007	0.1109	3.4
600	550	42.3	0.0431	0.0259	0.0439	5.1
840	550	7900	0.0001	0.0001	0.1117	5.7

$(0.11/2.82 \times 10^8)(\mathrm{GeV}/m_2)$.[4] If one neglects the p-wave contributions to $<\sigma v>$, one finds $\sigma^0_{0,2} = 2.03, 2.06, 2.09$ for $m_2 = 500, 700, 900$ GeV, respectively, where $\sigma^0_{0,2}$ is defined as $<\sigma(22;X)v>^0 = \sigma^0_{0,2} \times 10^{-9}$ GeV$^{-2} \simeq 1.16\ \sigma^0_{0,2} \times 10^{-26}$ cm^3/s (see Eq. (13)).

A large effective boost factor means large $\sigma_{0,ijk}$. Since each semi-annihilation (3) produces a DM particle, the cross section for the semi-annihilation can be larger than that for the standard annihilation process (1). To get an idea on the size of $<\sigma(ij;kX)v>$, we first consider the symmetric case, i.e., $\sigma_{0,123} = \sigma_{0,231} = \sigma_{0,312}$. In Table I we give the effective boost factor BF_X for various values of $\sigma_{0,123}, m_2$ and m_3 with the value of m_1 fixed at 1000 GeV. These values are chosen such that the sum of the individual relic abundances is consistent with $\Omega_T h^2 = 0.1126 \pm 0.0036$. As we see from Table I, the effective boost factor BF_X becomes large if the mass difference $m_1 - m_3$ is large and m_2 is close to m_1. But BF_X is at most of O(few), which would not be sufficient to explain the observed positron excess.

Next we consider the asymmetric case, i.e., $\sigma_{0,123} \neq \sigma_{0,231} \neq \sigma_{0,312}$. The reason why we can not obtain a large boost factor in the symmetric case is that, as we see from Table I, $Y_{i,\infty} \times Y_{j,\infty}$ for $i \neq j$ are small. Therefore, to suppress $\Omega_{\chi_3}h^2$ and the same time to increase $\Omega_{\chi_{1,2}}h^2$, we consider the situation $\sigma_{0,123} < \sigma_{0,231}, \sigma_{0,312}$. In Table II we give some examples of the asymmetric case, which show that it is in fact possible to obtain a boost factor BF_X of $O(10)$.

III. A MODEL WITH THREE DARK MATTER PARTICLES

We extend the original radiative seesaw model of [31] so as to have an additional discrete symmetry Z_2'. This can be done by introducing a SM singlet Majorana fermion χ and a SM singlet real inert scalar ϕ in addition to the inert Higgs doublet η which is present in the original model. The matter content of the model with the corresponding quantum numbers is given in Table III.

[4] We use $Y^0_2(x_\infty = 170)$ as $Y^0_{2,\infty}$.

TABLE II: The effective boost factor BF_X (19) for the asymmetric case, i.e., $\sigma_{0,123} \neq \sigma_{0,231} \neq \sigma_{0,312}$, with $m_1 = 1000$ GeV, $m_2 = 900$ GeV and $m_3 = 550$ GeV.

$\sigma_{0,123}$	$\sigma_{0,231}$	$\sigma_{0,312}$	$\Omega_{\chi_1}h^2$	$\Omega_{\chi_2}h^2$	$\Omega_{\chi_3}h^2$	BF_X
48.0	2000.0	48.4	0.0325	0.0007	0.0793	14.5
55.5	65.0	2000.0	0.0003	0.1118	0.0002	13.6
90.0	1000.0	100.3	0.0121	0.0011	0.0988	13.6
110.0	1000.0	125.3	0.0091	0.0010	0.1022	13.0
110.0	800.0	133.0	0.0080	0.0012	0.1032	12.3
110.0	600.0	145.2	0.0067	0.0015	0.1039	11.3

TABLE III: The matter content of the model and the corresponding quantum numbers. $Z_2 \times Z_2'$ is the unbroken discrete symmetry. The quarks are suppressed in the Table.

field	$SU(2)_L$	$U(1)_Y$	Z_2	Z_2'
(ν_{Li}, l_i)	2	$-1/2$	$+$	$+$
l_i^c	1	1	$+$	$+$
N_i^c	1	0	$-$	$+$
$H = (H^+, H^0)$	2	1/2	$+$	$+$
$\eta = (\eta^+, \eta^0)$	2	1/2	$-$	$+$
χ	1	0	$+$	$-$
ϕ	1	0	$-$	$-$

The $Z_2 \times Z_2'$ invariant Yukawa couplings of the lepton sector are given by

$$\mathcal{L}_Y = Y_{ij}^e H^\dagger L_i l_j^c + Y_{ik}^\nu L_i \epsilon \eta N_k^c + Y_k^\chi \chi N_k^c \phi + h.c. \ , \tag{20}$$

and the Majorana mass terms of the right-handed neutrinos N_k^c ($k = 1, 2, 3$) and the singlet fermion χ are[5]

$$\mathcal{L}_{\rm Maj} = \frac{1}{2} M_k N_k^c N_k^c + \frac{1}{2} M_\chi \chi^2 + h.c. \tag{21}$$

We may assume without loss of generality that the right handed neutrino mass matrix is diagonal and real. As far as the light neutrino masses, which are generated radiatively, are concerned, the last additional interaction term in Eq. (20) has no influence. So the neutrino phenomenology is the same as in the original model. The most general form of the $Z_2 \times Z_2'$

[5] A similar model is considered in [11].

invariant scalar potential can be written as

$$\begin{aligned} V &= m_1^2 H^\dagger H + m_2^2 \eta^\dagger \eta + \frac{1}{2} m_3^2 \phi^2 \\ &+ \frac{1}{2}\lambda_1 (H^\dagger H)^2 + \frac{1}{2}\lambda_2 (\eta^\dagger \eta)^2 + \lambda_3 (H^\dagger H)(\eta^\dagger \eta) + \lambda_4 (H^\dagger \eta)(\eta^\dagger H) \\ &+ \frac{1}{2}\lambda_5 [(H^\dagger \eta)^2 + h.c.] + \frac{1}{4!}\lambda_6 \phi^4 + \frac{1}{2}\lambda_7 (H^\dagger H)\phi^2 + \frac{1}{2}\lambda_8 (\eta^\dagger \eta)\phi^2 \ , \end{aligned} \tag{22}$$

from which we obtain the masses of the inert Higgs fields:

$$m_{\eta^\pm}^2 = m_2^2 + \lambda_3 v^2/2 \tag{23}$$

$$m_{\eta_R^0}^2 = m_2^2 + (\lambda_3 + \lambda_4 + \lambda_5) v^2/2 = m_2^2 + \lambda_L v^2/2 \tag{24}$$

$$m_{\eta_I^0}^2 = m_2^2 + (\lambda_3 + \lambda_4 - \lambda_5) v^2/2 \ , \tag{25}$$

$$m_\phi^2 = m_3^2 + \lambda_7 v^2/2 \ . \tag{26}$$

Here, $\langle H \rangle = v/\sqrt{2}$ is the Higgs VEV, and $\eta^0 = (\eta_R^0 + i\eta_I^0)/\sqrt{2}$. At this stage we have assumed that

$$\langle H \rangle = v/\sqrt{2}, \langle \eta \rangle = \langle \phi \rangle = 0 \tag{27}$$

correspond to the absolute minimum. (The sufficient condition for the absolute minimum of Eq. (22) is given below.) As we can see from Table III, the cold DM candidates are $N_k^c, \eta_R^0, \eta_I^0, \chi$ and ϕ, where η_R^0 as dark matter in the original model has been discussed in detail in [51–53]. To proceed, we assume that the mass relations

$$M_k >> m_{\eta^\pm}, m_{\eta_I^0} > m_{\eta_R^0} > m_\phi, m_\chi \text{ and } m_{\eta_R^0} < m_\phi + m_\chi \tag{28}$$

are satisfied.[6] These relations are chosen because we would like to meet the following requirements:

1. $\underline{\mu \to e\,\gamma}$

The constraint coming from $\mu \to e\gamma$ is given by [64]

$$B(\mu \to e\gamma) = \frac{3\alpha}{64\pi (G_F m_{\eta^\pm}^2)^2} \left| \sum_k Y_{\mu k}^\nu Y_{ek}^\nu F_2\left(\frac{M_k^2}{m_{\eta^\pm}^2}\right) \right|^2 \lesssim 2.4 \times 10^{-12} \ , \tag{29}$$

$$F_2(x) = \frac{1}{6(1-x)^4}(1 - 6x + 3x^2 + 2x^3 - 6x^2 \ln x) \ ,$$

where the upper bound is taken from [65]. A similar, but slightly weaker bound for $\tau \to \mu(e)\gamma$ given in [65] has to be satisfied, too. Since $F_2(x) \sim 1/3x$ for $x >> 1$, while $1/12 < F_2(x) < 1/6$ for $0 < x < 1$, the constraint can be readily satisfied if $M_k << m_{\eta^\pm}$ or $M_k >> m_{\eta^\pm}$.

[6] The possibility $m_{\eta_I^0} < m_{\eta_R^0}$ does not give any new feature of the model.

2. $g_\mu - 2$

The extra contribution to the anomalous magnetic moment of the muon, $a_\mu = (g_\mu - 2)/2$, is given by [64]

$$\delta a_\mu \;=\; \frac{m_\mu^2}{16\pi^2 m_{\eta^\pm}^2} \sum_k Y_{\mu k}^\nu Y_{\mu k}^\nu F_2\left(\frac{M_k^2}{m_{\eta^\pm}^2}\right) \;. \tag{30}$$

If we assume that $|\sum_k Y_{\mu k}^\nu Y_{\mu k}^\nu F_2\left(\frac{M_k^2}{m_{\eta^\pm}^2}\right)| \simeq |\sum_k Y_{\mu k}^\nu Y_{ek}^\nu F_2\left(\frac{M_k^2}{m_{\eta^\pm}^2}\right)|$, then we obtain

$$|\delta a_\mu| \;\simeq\; 2.2\times 10^{-5} B(\mu\to e\gamma) \lesssim 3.4\times 10^{-11} \tag{31}$$

if Eq. (29) is satisfied, where the upper bound is taken from [66]. So, the constraint from a_μ has no significant influence.

3. Stable and global minimum

The DM stabilizing symmetry Z_2 remains unbroken if

$$\begin{aligned} &m_1^2 < 0 \;,\; m_2^2 > 0 \;,\; m_3^2 > 0 \;, \\ &\lambda_1 \;,\; \lambda_2 \;,\; \lambda_6 > 0 \;,\; \lambda_3 + \lambda_4 - |\lambda_5|, \lambda_3 > -\frac{1}{2}(\lambda_1\lambda_2)^{1/2} \;, \\ &\lambda_7 > -\frac{1}{2}(\lambda_1\lambda_6/3)^{1/2} \;,\; \lambda_8 > -\frac{1}{2}(\lambda_2\lambda_6/3)^{1/2} \end{aligned} \tag{32}$$

are satisfied. These conditions are sufficient for Eq. (27) to correspond to the absolute minimum. Since $m_{\eta_R^0}^2 - m_{\eta_I^0}^2 = \lambda_5 v^2$, a negative λ_5 is consistent with Eq. (28).

4. Electroweak precision

The electroweak precision measurement requires [51, 66]

$$\Delta T \;\simeq\; 0.54 \left(\frac{m_{\eta^\pm} - m_{\eta_R^0}}{v}\right)\left(\frac{m_{\eta^\pm} - m_{\eta_I^0}}{v}\right) = 0.02^{+0.11}_{-0.12} \tag{33}$$

for $m_h = 115 - 127$ GeV. Therefore, $|m_{\eta^\pm} - m_{\eta_R^0}| \;,\; |m_{\eta^\pm} - m_{\eta_I^0}| \lesssim 100$ GeV is sufficient to meet the requirement.

Then, with the assumption of the above mass relations, we look at the radiative neutrino mass matrix [31]

$$\begin{aligned} (\mathcal{M}_\nu)_{ij} \;&=\; \sum_k \frac{Y_{ik}^\nu Y_{jk}^\nu M_k}{16\pi^2}\left[\; \frac{m_{\eta_R^0}^2}{m_{\eta_R^0}^2 - M_k^2}\ln\left(\frac{m_{\eta_R^0}}{M_k}\right)^2 - \frac{m_{\eta_I^0}^2}{m_{\eta_I^0}^2 - M_k^2}\ln\left(\frac{m_{\eta_I^0}}{M_k}\right)^2 \;\right] \\ &\simeq\; -\sum_k \frac{Y_{ik}^\nu Y_{jk}^\nu}{16\pi^2}\left[\frac{m_{\eta_R^0}^2}{M_k}\ln\left(\frac{m_{\eta_R^0}}{M_k}\right)^2 - \frac{m_{\eta_I^0}^2}{M_k}\ln\left(\frac{m_{\eta_I^0}}{M_k}\right)^2\right] \;\text{ for } m_{\eta_R^0}, m_{\eta_I^0} << M_k \;. \end{aligned} \tag{34}$$

Since $(\mathcal{M}_\nu)_{ij}$ are of order 10^{-1} eV and $m_{\eta_R^0}^2 - m_{\eta_I^0}^2 = \lambda_5 v^2$, we need $\sum_k Y_{ik}^\nu Y_{jk}^\nu \lesssim O(10^{-9})$ for $|\lambda_5| \gtrsim O(0.1)$. Note, however, that this does not automatically imply that $\sum_{i,k}^3 |Y_{ik}^\nu|^2 \lesssim O(10^{-9})$, and in fact it could be much larger if we assume a specific flavor structure of Y_{jk}^ν. If there exists another source for the neutrino mass matrix, we have to add it to (34).

A. Relic abundance of dark matter

Now we come to the relic abundance of DM. Under the assumption about the mass relations (28) we have to consider the following annihilation processes:[7]

$$\bullet \eta_R^0\ \eta_R^0 \leftrightarrow \text{SMs}\ ,\quad \bullet\ \phi\ \phi \leftrightarrow \text{SMs (Standard annihilation)} \tag{35}$$

$$\bullet \eta_R^0\ \eta_R^0 \leftrightarrow \phi\ \phi\ ,\quad \bullet\ \chi\ \chi \leftrightarrow \phi\ \phi \text{ (Conversion)} \tag{36}$$

$$\bullet \eta_R^0\ \chi \leftrightarrow \phi\ \nu_L\ ,\quad \bullet \chi\ \phi \leftrightarrow \eta_R^0\ \nu_L\ ,\quad \bullet\ \phi\ \eta_R^0 \leftrightarrow \chi\ \nu_L \text{ (Semi-annihilation)} \tag{37}$$

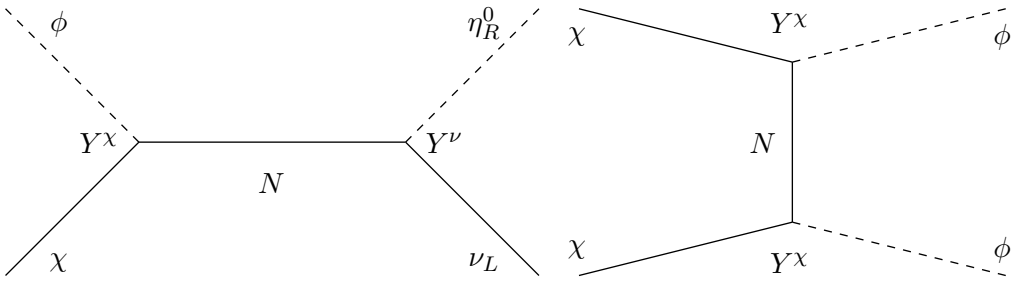

FIG. 6: Semi-annihilation diagram (left) and conversion (right).

We have yet not specified the relative size of m_χ and m_ϕ. If χ is lighter than ϕ, the conversion of χ into ϕ is kinematically forbidden and the semi-annihilation in Fig. 6 is the only kinematically allowed annihilation for χ. So, we will consider below only the case $m_\chi > m_\phi$. First we consider a benchmark set of the input parameter values:

$$\begin{aligned}
m_{\eta_R^0} &= 200 \text{ GeV}\ ,\ m_\chi = 190 \text{ GeV}\ ,\ m_\phi = 180 \text{ GeV}\ ,\\
m_{\eta^\pm} &= m_{\eta_I^0} = 210 \text{ GeV}\ ,\\
m_h &= 125 \text{ GeV}\ ,\ M_1 = M_2 = M_3 = 1000 \text{ GeV}\ ,\\
\lambda_3 &= -0.065\ ,\ \lambda_7 = 0.1\ ,\ \lambda_8 = 0.1\ ,\ \lambda_L = -0.2\ ,\\
\sum_{k=1}^{3} |Y_k^\chi|^2 &= 3(0.7)^2\ ,\ \sum_{i,k=1}^{3} |Y_{ik}^\nu|^2 = 9(0.01)^2\ .
\end{aligned} \tag{38}$$

With this choice of the parameter values we obtain

$$\begin{aligned}
<\sigma(\eta_R^0\eta_R^0;\text{SMs})v> &= 45.66 - 38.21/x\ ,\ \ <\sigma(\phi\phi;\text{SMs})v> = 5.93 - 1.92/x\ \ ,\\
<\sigma(\eta_R^0\eta_R^0;\phi\phi)v> &= 0.46 + 0.29/x\ ,\ \ <\sigma(\chi\chi;\phi\phi)v> = 0 + 77.18/x\ ,\\
<\sigma(\chi\eta_R^0;\phi\nu_L)v> &= 0.02 + 0.01/x\ ,\ \ <\sigma(\eta_R^0\phi;\chi\nu_L)v> = 0.07 + 0.02/x\ ,\\
<\sigma(\chi\phi;\eta_R^0\nu_L)v> &= 0.07 + 0.04/x
\end{aligned} \tag{39}$$

[7] We neglect the coannihilations such as that of η_R^0 with η_I^0 and $\eta^\pm$ below.

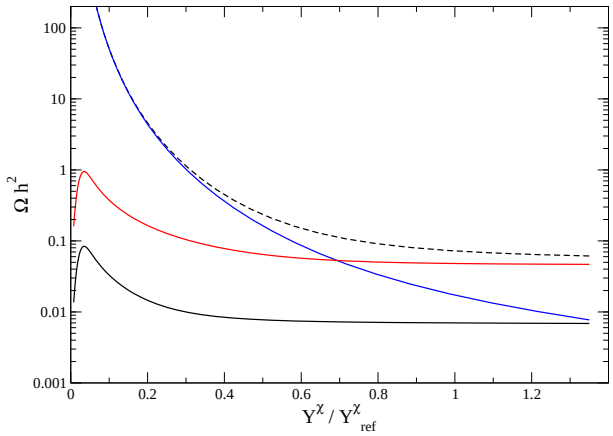

FIG. 7: Y^χ dependence of the relic abundances, $\Omega_T h^2$ (dashed), $\Omega_\eta h^2$ (black), $\Omega_\chi h^2$ (blue), $\Omega_\phi h^2$ (red), where Y^χ controls the size of the semi-annihilation and conversion shown in Fig. 6. The input parameter values are given in Eq. (38).

in units of 10^{-9} GeV^{-2}, and

$$\Omega_T h^2 \;=\; 0.1094 \;,\; \Omega_\eta h^2 = 0.0062 \;,\; \Omega_\chi h^2 = 0.0511 \;,\; \Omega_\phi h^2 = 0.0521 \;, \tag{40}$$

where $x = (1/m_{\eta_R^0} + 1/m_\chi + 1/m_\phi)^{-1}/T = \mu/T$. As we see from Fig. 6, the size of the semi-annihilation and conversion is controlled by Y_k^χ. In Fig. 7 we show the Y^χ dependence of the individual abundances, where we have varied $\sum_k |Y_k^\chi|^2$, and $Y^\chi/Y^\chi_{\rm ref}$ stands for $\left(\sum_k |Y_k^\chi|^2/3(0.7)\right)^{1/2}$. If $Y^\chi/Y^\chi_{\rm ref} << 1$, the conversion of χ and the semi-annihilations $\chi\ \phi \to \eta_R^0\ \nu_L$, $\chi\ \eta_R^0 \to \phi\ \nu_L$ become small, such that $\Omega_\chi h^2$ in particular increases.

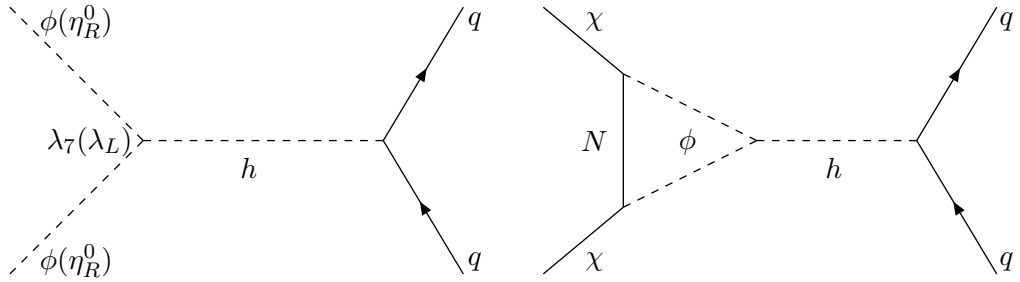

FIG. 8: Tree (left) and one-loop (right) level interactions with the quarks.

B. Imposing constraints

To be more realistic, we have to impose constraints from direct detection, collider experiments, and perturbativity, $|\lambda_i|, |Y^\nu_{ij}|, |Y^\chi_i| < 1$, in addition to Eqs. (29)–(33), which we shall

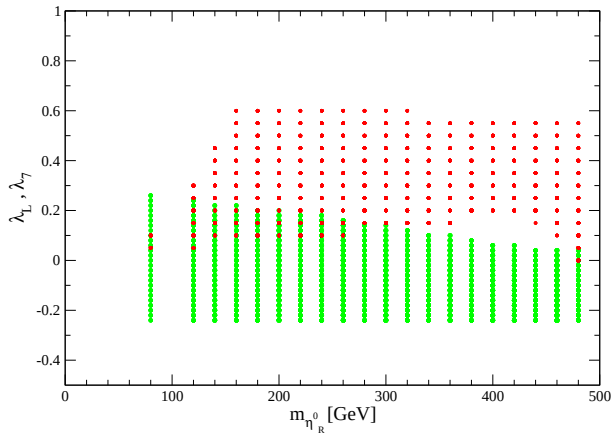

FIG. 9: The allowed regime in the $\lambda_L(\lambda_7)-m_{\eta^0_R}$ plane for $(\delta_1 = 10\ ,\ \delta_2 = 10)$ GeV with $m_\chi = m_{\eta^0_R} - 10$ GeV, $m_\phi = m_{\eta^0_R} - 20$ GeV and $M_k = 1000$ GeV. The green and red points are for λ_L and λ_7, respectively.

do next. ϕ and η^0_R have tree-level interactions to the quarks which are shown in Fig. 8.[8] In the following discussions we ignore the one-loop contributions such as the right diagram in Fig. 8.[9] The spin-independent elastic cross section off the nucleon $\sigma(\phi(\eta^0_R))$ is given by [51]

$$\sigma(\phi(\eta^0_R)) \ = \ \frac{1}{4\pi}\left(\frac{\lambda_{7(L)}\hat{f} m_N}{m_{\phi(\eta^0_R)} m_h^2}\right)^2 \left(\frac{m_N m_{\phi(\eta^0_R)}}{m_N + m_{\phi(\eta^0_R)}}\right)^2 \ , \tag{41}$$

where m_N is the nucleon mass, and $\hat{f} \sim 0.3$ stems from the nucleonic matrix element [72]. The cross sections have to satisfy

$$\left(\frac{\sigma(\phi)}{\sigma_{\rm UB}(m_\phi)}\right)\left(\frac{\Omega_\phi h^2}{0.112}\right) + \left(\frac{\sigma(\eta^0_R)}{\sigma_{\rm UB}(m_{\eta^0_R})}\right)\left(\frac{\Omega_\eta h^2}{0.112}\right) \lesssim 1 \ , \tag{42}$$

where $\sigma_{\rm UB}(m)$ is the current experimental limit on the cross section for the DM mass m.

In the absence of χ and ϕ, the lower mass region 60 GeV $\lesssim m_{\eta^0_R} \lesssim$ 80 GeV is consistent with all the experimental constraints [53].[10] But the elastic cross section $\sigma(\eta^0_R) \simeq 7.9 \times 10^{-45}(\lambda_L/0.05)^2(60\ {\rm GeV}/m_{\eta^0_R})^2\ {\rm cm}^2$ with $\lambda_L \gtrsim 0.05$ in this mass range may exceed the upper bound of the XENON100 result [73],[11] 7.0×10^{-45} cm^2 for the DM mass 50 GeV at 90 C.L. The higher mass region, i.e., $m_{\eta^0_R} \gtrsim 500$ GeV with $\sigma(\eta^0_R) \simeq 4.6 \times 10^{-46}(\lambda_L/0.1)^2(500\ {\rm GeV}/m_{\eta^0_R})^2\ {\rm cm}^2$, will be significant for next generation experiments such as SuperCDMS [80], XENON1T [81] or XMASS [82].

The presence of χ and ϕ changes the situation. Firstly, the separation of two allowed regions of $m_{\eta^0_R}$ disappears: As far as the relic abundance is concerned, $m_{\eta^0_R}$ is allowed

[8] Direct detection of two DM particles has been discussed for instance in [8, 17, 18, 21]. LHC signals of η dark matter have been discussed in [51, 67, 68]. See also [11, 18].

[9] There exist also one-loop corrections to $\eta^0_R q \to \eta^0_R q$ [69]. See also [70].

[10] There exists a marginal possibility to expend slightly this upper bound [71].

[11] See also [74]–[79].

between 80 and 500 GeV, too, as we have seen, because χ and ϕ also contribute to the relic abundance. Secondly, the parameter space becomes considerably larger. To see how the allowed parameter space of the model without χ and ϕ changes, we consider a set of $(\delta_1 = m_{\eta^\pm} - m_{\eta_R^0}\ ,\ \delta_2 = m_{\eta_I^0} - m_{\eta_R^0})$, for which the allowed parameter space without χ and ϕ is very small. For $(\delta_1 = 10\ ,\ \delta_2 = 10)$ GeV, for instance, there is no allowed range of $m_{\eta_R^0} \lesssim 500$ GeV [53]; the low mass range of $m_{\eta_R^0}$, for which the relic abundance $\Omega_\eta h^2$ is consistent, does not satisfy the LEP constraint. Below we show how this situation changes in the presence of χ and ϕ. The LEP constraint implies that the region satisfying $m_{\eta_R^0} \lesssim 80$ GeV and $m_{\eta_I^0} \lesssim 100$ GeV with $\delta_2 \gtrsim 8$ GeV is excluded [53]. Therefore, for $(\delta_1 = 10\ ,\ \delta_2 = 10)$ GeV we have to consider only $m_{\eta_R^0} > 80$ GeV. Further, to suppress the parameter space we assume that $m_\chi = m_{\eta_R^0} - 10$ GeV, $m_\phi = m_{\eta_R^0} - 20$ GeV and $M_k = 1000$ GeV, and we scan $m_{\eta_R^0}$ from 80 to 500 GeV.

Fig. 9 shows the allowed area in the $\lambda_L(\lambda_7) - m_{\eta_R^0}$ plane, where all the constraints are taken into account. The allowed mass range for $m_{\eta_R^0}$ is extended as expected. The reason why there are no allowed points around $m_{\eta_R^0} \simeq 100$ GeV is the following. Since we keep the mass difference fixed, we have $m_\phi = m_{\eta_R^0} - 20 \simeq 80$ GeV there. This is the threshold regime for the process $\phi\phi \to W^+W^-$. So, for $m_{\eta_R^0}$ just below 100 GeV, the annihilation cross section for ϕ is small because of small λ_7 in this range of m_ϕ, and therefore the relic abundance $\Omega_\phi h^2$ exceeds 0.12. We see that $m_{\eta_R^0} = 80$ GeV is allowed on the other hand. This allowed area exists, though λ_7 is small, because around $m_\phi = 62$ GeV the s-channel annihilation of ϕ becomes resonant due to $m_h = 125$ GeV. For $m_{\eta_R^0}$ just above 100 GeV, the annihilation cross section for ϕ is large because the channel to W^+W^- is now open, so that $\Omega_\phi h^2$ can not supplement the anyhow small $\Omega_\eta h^2$.

If we suppress the constraint from the direct detection, we have a prediction on the direct detection. Fig. 10 shows the spin-independent cross section off the nucleon versus the DM mass; the green area for the η DM and the violet area for the ϕ DM. We see that the the spin-independent cross sections are not only consistent with the current bound of XENON100 [73], but also are within the accessible range of future experiments.

C. Indirect detection

If DM annihilates sufficiently into SM particles, the resulting cosmic rays may be observable. These are indirect signals of DM, and in fact excesses in e^+ [41]–[44] and in γ [83]–[86] have been recently reported. Indirect detection of DM has been studied within the framework of a two component DM system in [7, 9, 12–14, 17, 25, 26], and also of the inert Higgs model in [52, 87–89]. As we see from the semi-annihilation diagram in Fig. 6, the process produces only a left-handed neutrino as the SM particle. Therefore, the boost factor to enhance the annihilation cross section to obtain an excess in e^+ is not available in this model. So, we are particularly interested in the neutrinos from the annihilation of captured DM in

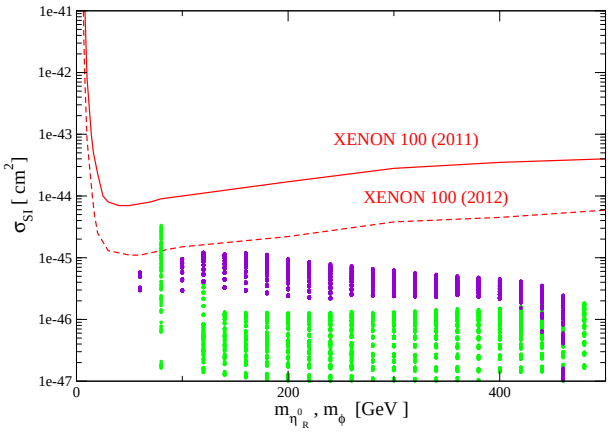

FIG. 10: The spin-independent cross section off the nucleon is plotted as a function of the DM mass. The green and violet areas are for η and ϕ DM's, respectively, where we have used ($\delta_1 = 10$, $\delta_2 = 10$) GeV with $m_\chi = m_{\eta_R^0} - 10$ GeV, $m_\phi = m_{\eta_R^0} - 20$ GeV and $M_k = 1000$ GeV.

the Sun [54]–[63] (see [4, 5] for a review, and [89] for the case of the inert Higgs model), because (i) the semi-annihilation produces a monochromatic neutrino ($E_\nu \simeq m_{\eta_R^0} + m_\phi - m_\chi$ for instance) in addition to those with $E_\nu \simeq m_{\eta_R^0}$ along with the continuum spectrum, (ii) these neutrinos can be observed at neutrino telescopes [90–92], and (iii) the evolution equations of the DM numbers in the Sun, which describe approaching equilibrium between the capture and annihilation (including conversion and semi-annihilation) rates of DM, are coupled now.

We denote the number of DM particles η, χ and ϕ in the Sun by N_i with $i = \eta, \chi$ and ϕ, respectively. Then the change of N_i with respect to time t is given by

$$\begin{aligned}
\dot{N}_\eta &= C_\eta - C_A(\eta\eta \leftrightarrow \mathrm{SM})N_\eta^2 - C_A(\eta\eta \leftrightarrow \phi\phi)N_\eta^2 - C_A(\eta\chi \leftrightarrow \phi\nu_L)N_\eta N_\chi \\
&\quad - C_A(\eta\phi \leftrightarrow \chi\nu_L)N_\eta N_\phi + C_A(\phi\chi \leftrightarrow \eta\nu_L)N_\chi N_\phi \ , \qquad (43) \\
\dot{N}_\chi &= C_\chi - C_A(\chi\chi \leftrightarrow \phi\phi)N_\chi^2 - C_A(\eta\chi \leftrightarrow \phi\nu_L)N_\eta N_\chi \\
&\quad + C_A(\eta\phi \leftrightarrow \chi\nu_L)N_\eta N_\phi - C_A(\phi\chi \leftrightarrow \eta\nu_L)N_\chi N_\phi \ , \qquad (44) \\
\dot{N}_\phi &= C_\phi - C_A(\phi\phi \leftrightarrow \mathrm{SM})N_\phi^2 + C_A(\eta\eta \leftrightarrow \phi\phi)N_\eta^2 + C_A(\chi\chi \leftrightarrow \phi\phi)N_\chi^2 \\
&\quad + C_A(\eta\chi \leftrightarrow \phi\nu_L)N_\eta N_\chi - C_A(\eta\phi \leftrightarrow \chi\nu_L)N_\eta N_\phi - C_A(\phi\chi \leftrightarrow \eta\nu_L)N_\chi N_\phi \ , \qquad (45)
\end{aligned}$$

where the C_i's are the capture rates in the Sun and the C_A's are proportional to the annihilation cross sections times the relative DM velocity per volume in the limit $v \to 0$:

$$\begin{aligned}
C_{\phi(\eta)} &\simeq 1.4 \times 10^{20} f(m_{\phi(\eta_R^0)}) \left(\frac{\hat{f}}{0.3}\right)^2 \left(\frac{\lambda_{7(L)}}{0.1}\right)^2 \left[\frac{m_h}{125\ \mathrm{GeV}}\right]^{-4} \\
&\quad \times \left(\frac{200\ \mathrm{GeV}}{m_{\phi(\eta_R^0)}}\right)^2 \left(\frac{\Omega_{\phi(\eta)}h^2}{0.112}\right) \mathrm{s}^{-1} \ , \ C_\chi = 0 \ , \qquad (46)
\end{aligned}$$

where the function $f(m_{\phi(\eta_R^0)})$ depends on the form factor of the nucleus, elemental abundance, kinematic suppression of the capture rate, etc, varying from $O(1)$ to $O(0.01)$ depend-

ing on the DM mass [60, 61]. The annihilation rates C_A can be calculated from [58]

$$C_A(ij \leftrightarrow \bullet) \;=\; \frac{<\sigma(ij;\bullet)v>}{V_{ij}} \;,\; V_{ij} = 5.7\times 10^{27}\left(\frac{100\ \mathrm{GeV}}{\mu_{ij}}\right)^{3/2}\mathrm{cm}^3\,, \tag{47}$$

with $\mu_{ij} = 2m_im_j/(m_i+m_j)$ in the limit $v \to 0$.

There are fixed points of the evolution equations, which correspond to equilibrium. Since at the time of birth of the Sun the numbers N_i were zero, the N_i increase with time and approach the fixed point values, i.e., equilibrium at which N_i assumes its maximal value. So, the question is whether the age of the Sun, $t_\odot \simeq 4.5\times 10^9$ years, is old enough for N_i to reach equilibrium. We see from the evolution equations that the fixed point values are roughly proportional to $(C_i/C_A)^{1/2}$, implying that we need large capture rates C_i to obtain large $N_i(t_\odot)$. The annihilation, conversion and semi-annihilation rates at $t = t_\odot$ are given by

$$\Gamma(ij;\bullet) \;=\; d_{ij}C_A(ij \leftrightarrow \bullet)N_i(t_\odot)N_j(t_\odot)\;, \tag{48}$$

where $d_{ii} = 1/2$ and $d_{ij} = 1$ for $i \neq j$. The observation rate of the neutrinos $\Gamma_{\rm detect}$ is proportional to $\Gamma(ij;\bullet)$. As a benchmark we use the same set of the input parameter values as (38). In Fig. 11 we show the time evolution of[12]

$$\Gamma(\mathrm{SM}) \;=\; C_A(\eta\eta \leftrightarrow \mathrm{SM})N_\eta^2/2 + C_A(\phi\phi \leftrightarrow \mathrm{SM})N_\phi^2/2\;, \tag{49}$$

$$\Gamma(\nu) \;=\; C_A(\eta\phi \leftrightarrow \chi\nu)N_\eta N_\phi + C_A(\eta\chi \leftrightarrow \phi\nu)N_\eta N_\chi + C_A(\chi\phi \leftrightarrow \eta\nu)N_\chi N_\phi\;, \tag{50}$$

$$\Gamma(\nu\nu) \;=\; C_A(\eta\eta \leftrightarrow \nu\nu)N_\eta^2/2\;, \tag{51}$$

scaled to 10^{20} s^{-1}, as function of $\tau = t/t_\odot$. As we see from Fig. 11, the rates seem to be saturated: $\Gamma(\mathrm{SM})$ is in fact saturated, but $\Gamma(\nu)$ does not reach its fixed-point value 0.002×10^{20} s^{-1} at $\tau = t/t_\odot = 1$. The saturated value of $\Gamma(\mathrm{SM})$ is 0.28×10^{20} s^{-1} for the input parameters (38), which is consistent with the upper limit $\sim 2.73\times 10^{21}$ s^{-1} for $m_{\rm DM} =$ 250 GeV of the AMANDA-II / IceCube neutrino telescope [90]. As for the monochromatic neutrinos we obtain $\Gamma(\nu) = 1.1\times 10^{-3}\times 10^{20}$ s^{-1} and $\Gamma(\nu\nu) = 1.3\times 10^{-7}\times 10^{20}$ s^{-1}. To estimate the detection rate $\Gamma_{\rm detect}$ we use the formula [93]

$$\Gamma_{\rm detect} = AP(E_\nu)\Gamma_{\rm inc}\;, \tag{52}$$

where A is the detector area facing the incident beam, $P(E_\nu)$ is the probability for detection as a function of the neutrino energy $P(E_\nu)$, and $\Gamma_{\rm inc} = \Gamma/4\pi R_\odot^2$ is the incoming neutrino flux, i.e., the number of neutrinos per unit area per second on the Earth ($R_\odot$ is the distance

[12] For the monochromatic neutrinos, i.e. $\Gamma(\nu)$, we have added all the semi-annihilations, because for the mass values given in (38) the neutrino energies are all closed to 200 GeV. Moreover, the first term in the r.h.s. of Eq. (50) (which counts neutrinos of $m_{\eta_R^0} + m_\phi - m_\chi = 190$ GeV) is a dominant contribution with about 95%.

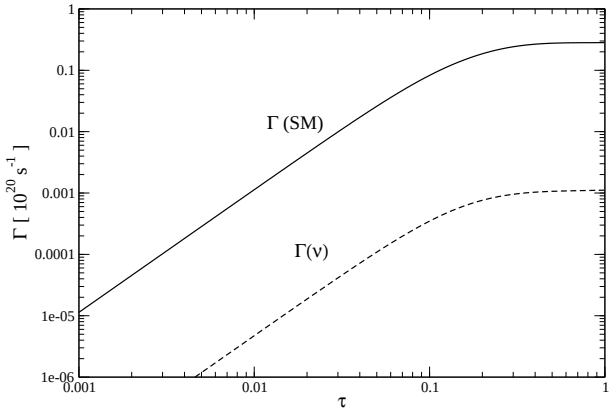

FIG. 11: The time evolution of the annihilation rates Γ(SM) and $\Gamma(\nu)$, where $\tau = t/t_\odot$, and the input parameter values are given in (38).

to the Sun $\simeq 1.5 \times 10^8$ km).[13] The probability $P(E_\nu)$ may be approximated as the ratio of the effective detector length L to the mean free path of the neutrinos in the detector. For the neutrinos (anti-neutrinos) one finds: $P(E_{\nu(\bar{\nu})}) \simeq 2.0(1.0) \times 10^{-11}(L/\text{km})(E_{\nu(\bar{\nu})}/\text{GeV})$, arriving at

$$\Gamma_{\text{detect}} \simeq 2.2(1.1) \times 10^{-21} \left(\frac{A}{\text{km}^2}\right) \left(\frac{L}{\text{km}}\right) \left(\frac{E_{\nu(\bar{\nu})}}{\text{GeV}}\right) \left(\frac{\Gamma}{\text{s}^{-1}}\right) \text{yr}^{-1} , \tag{53}$$

which implies that, for the input parameters of (38), 0.05 events of monochromatic neutrinos with $\sim$ 200 GeV per year may be detected at IceCube [90], we have used: $A = 1\text{km}^2$, $L = 1\text{km}$.

0.05 events per year may be too small to be realistic. However, we would like to note that we have studied only one point in the whole parameter space. It will be our future program to implement the sophisticated method of [94] and to survey the whole parameter space. We also would like to note that if at least one of the fermionic DM in a multi-component DM system has odd parity of the discrete lepton number, a monochromatic left-handed neutrino, which is also odd, can be produced together with this fermionic DM in a semi-annihilation of DM's.

IV. CONCLUSION

We have considered the conversion and semi-annihilation of DM in a multi-component DM system. We have found that these non-standard DM annihilation processes can influence the relic abundance of DM a lot, which has been recently found for two-component DM systems in [16, 21, 22]. The question of whether a large boost factor can be obtained within the

[13] A sophisticated method to compute the observation rates at IceCube was recently developed in [94].

framework of thermally produced DM in a three-component DM system has been addressed. It has turned out that a boost factor of at most $O(10)$ can be obtained.

As a concrete three-component DM system we have considered a radiative seesaw model of [31], which is extended to include an extra Majorana fermion χ and an extra real scaler boson ϕ. The DM stabilizing symmetry is promoted to $Z_2 \times Z_2'$, and we have assumed that η_R^0 (the CP even neutral component of the inert Higgs $SU(2)_L$ doublet), χ and ϕ are DM. We have shown that the previously found separation [51–53] of the allowed parameter space in the low and high mass regions for η_R^0 disappears in the presence of χ and ϕ.

Finally, we have discussed neutrinos coming from the annihilations of the captured DM in the Sun. The evolution equations of the DM numbers in the Sun, which describe approaching equilibrium between the capture and annihilation (including conversion and semi-annihilation) rates of DM, are coupled in multi-component DM system. Due to the semi-annihilations of DM, monochromatic neutrinos are radiated, and the observation rates of neutrinos have been estimated. Observations of high energy monochromatic neutrinos from the Sun may indicate a multi-component DM system.

The work of M. D. is supported by the International Max Planck Research School for Precision Tests of Fundamental Symmetries. The work of M. A. is supported in part by Grant-in-Aid for Scientific Research for Young Scientists (B) (No.22740137), and J. K. is partially supported by Grant-in-Aid for Scientific Research (C) from Japan Society for Promotion of Science (No.22540271). M. D. thanks the Institute for Theoretical Physics at Kanazawa University for very kind hospitality.

---

[1] A. G. Riess *et al.* [Supernova Search Team Collaboration], "Observational Evidence from Supernovae for an Accelerating Universe and a Cosmological Constant," Astron. J. **116** (1998) 1009 [arXiv:astro-ph/9805201].

[2] K. N. Abazajian *et al.* [SDSS Collaboration], "The Seventh Data Release of the Sloan Digital Sky Survey," Astrophys. J. Suppl. **182** (2009) 543 [arXiv:0812.0649 [astro-ph]].

[3] E. Komatsu *et al.* [WMAP Collaboration], "Seven-Year Wilkinson Microwave Anisotropy Probe (WMAP) Observations: Cosmological Interpretation," Astrophys. J. Suppl. **192** (2011) 18 [arXiv:1001.4538 [astro-ph.CO]].

[4] G. Jungman, M. Kamionkowski, K. Griest, "Supersymmetric dark matter," Phys. Rept. **267** (1996) 195-373 [arXiv:hep-ph/9506380].

[5] G. Bertone, D. Hooper and J. Silk, "Particle dark matter: Evidence, candidates and constraints," Phys. Rept. **405** (2005) 279 [arXiv:hep-ph/0404175]; G. Bertone, (ed.), "Particle dark matter: Observations, models and searches," Cambridge University Press 2010.

[6] M. Cirelli, "Indirect Searches for Dark Matter: a status review," arXiv:1202.1454 [hep-ph].

[7] C. Boehm, P. Fayet, J. Silk, "Light and heavy dark matter particles," Phys. Rev. **D69** (2004) 101302 [arXiv:hep-ph/0311143].

[8] T. Hur, H.-S. Lee and S. Nasri, "A Supersymmetric U(1)-prime Model with Multiple Dark Matters," Phys. Rev. D **77** (2008) 015008 [arXiv:0710.2653 [hep-ph]].

[9] Q. H. Cao, E. Ma, J. Wudka and C. P. Yuan, "Multipartite dark matter," arXiv:0711.3881 [hep-ph].

[10] J. L. Feng and J. Kumar, "The WIMPless Miracle: Dark-Matter Particles without Weak-Scale Masses or Weak Interactions," Phys. Rev. Lett. **101** (2008) 231301 [arXiv:0803.4196 [hep-ph]].

[11] H. S. Cheon, S. K. Kang and C. S. Kim, "Doubly Coexisting Dark Matter Candidates in an Extended Seesaw Model," Phys. Lett. B **675** (2009) 203 [Erratum-ibid. B **698** (2011) 324] [arXiv:0807.0981 [hep-ph]].

[12] J.-H. Huh, J. E. Kim, B. Kyae, "Two dark matter components in dark matter extension of the minimal supersymmetric standard model and the high energy positron spectrum in PAMELA/HEAT data," Phys. Rev. **D79** (2009) 063529 [arXiv:0809.2601 [hep-ph]].

[13] M. Fairbairn and J. Zupan, "Dark matter with a late decaying dark partner," JCAP **0907** (2009) 001 [arXiv:0810.4147 [hep-ph]].

[14] K. M. Zurek, "Multi-Component Dark Matter," Phys. Rev. **D79** (2009) 115002 [arXiv:0811.4429 [hep-ph]].

[15] D. E. Morrissey, D. Poland and K. M. Zurek, "Abelian Hidden Sectors at a GeV," JHEP **0907** (2009) 050 [arXiv:0904.2567 [hep-ph]].

[16] F. D'Eramo and J. Thaler, "Semi-annihilation of Dark Matter," JHEP **1006** (2010) 109 [arXiv:1003.5912 [hep-ph]].

[17] D. Feldman, Z. Liu, P. Nath and G. Peim, "Multicomponent Dark Matter in Supersymmetric Hidden Sector Extensions," Phys. Rev. D **81** (2010) 095017 [arXiv:1004.0649 [hep-ph]].

[18] B. Batell, "Dark Discrete Gauge Symmetries," Phys. Rev. D **83** (2011) 035006 [arXiv:1007.0045 [hep-ph]].

[19] Z.-P. Liu, Y.-L. Wu and Y.-F. Zhou, "Enhancement of dark matter relic density from the late time dark matter conversions," Eur. Phys. J. C **71** (2011) 1749 [arXiv:1101.4148 [hep-ph]].

[20] K. R. Dienes and B. Thomas, "Dynamical Dark Matter: I. Theoretical Overview," Phys. Rev. D **85** (2012) 083523 [arXiv:1106.4546 [hep-ph]]; K. R. Dienes and B. Thomas, "Dynamical Dark Matter: II. An Explicit Model," Phys. Rev. D **85** (2012) 083524 [arXiv:1107.0721 [hep-ph]]; K. R. Dienes, S. Su and B. Thomas, "Distinguishing Dynamical Dark Matter at the LHC," arXiv:1204.4183 [hep-ph].

[21] G. Belanger and J.-C. Park, "Assisted freeze-out," JCAP **1203** (2012) 038 [arXiv:1112.4491 [hep-ph]].

[22] G. Belanger, K. Kannike, A. Pukhov and M. Raidal, "Impact of semi-annihilations on dark matter phenomenology - an example of Z_N symmetric scalar dark matter," JCAP **1204** (2012) 010 [arXiv:1202.2962 [hep-ph]].

[23] I. P. Ivanov and V. Keus, "Z_p scalar dark matter from multi-Higgs-doublet models," arXiv:1203.3426 [hep-ph].

[24] E. Ma, "Supersymmetric Model of Radiative Seesaw Majorana Neutrino Masses," Annales Fond. Broglie **31** (2006) 285 [arXiv:hep-ph/0607142]; E. Ma, "Supersymmetric U(1) Gauge Realization of the Dark Scalar Doublet Model of Radiative Neutrino Mass," Mod. Phys. Lett. **A23** (2008) 721 [arXiv:0801.2545 [hep-ph]].

[25] H. Fukuoka, J. Kubo and D. Suematsu, "Anomaly Induced Dark Matter Decay and PAMELA/ATIC Experiments," Phys. Lett. B **678** (2009) 401 [arXiv:0905.2847 [hep-ph]].

[26] H. Fukuoka, D. Suematsu and T. Toma, "Signals of dark matter in a supersymmetric two dark matter model," JCAP **1107** (2011) 001 [arXiv:1012.4007 [hep-ph]].

[27] D. Suematsu and T. Toma, "Dark matter in the supersymmetric radiative seesaw model with an anomalous U(1) symmetry," Nucl. Phys. B **847** (2011) 567 [arXiv:1011.2839 [hep-ph]].

[28] M. Aoki, J. Kubo, T. Okawa and H. Takano, "Impact of Inert Higgsino Dark Matter," Phys. Lett. B **707** (2012) 107 [arXiv:1110.5403 [hep-ph]].

[29] E. Ma, "Z(3) Dark Matter and Two-Loop Neutrino Mass," Phys. Lett. B **662** (2008) 49 [arXiv:0708.3371 [hep-ph]].

[30] K. Agashe, D. Kim, M. Toharia and D. G. E. Walker, "Distinguishing Dark Matter Stabilization Symmetries Using Multiple Kinematic Edges and Cusps," Phys. Rev. D **82** (2010) 015007 [arXiv:1003.0899 [hep-ph]].

[31] E. Ma, "Verifiable radiative seesaw mechanism of neutrino mass and dark matter," Phys. Rev. D **73** (2006) 077301 [arXiv:hep-ph/0601225].

[32] K. Griest, "Cross-Sections, Relic Abundance and Detection Rates for Neutralino Dark Matter," Phys. Rev. D **38** (1988) 2357 [Erratum-ibid. D **39** (1989) 3802].

[33] M. Srednicki, R. Watkins and K. A. Olive, "Calculations of Relic Densities in the Early Universe," Nucl. Phys. B **310** (1988) 693.

[34] K. Griest, M. Kamionkowski and M. S. Turner, "Supersymmetric Dark Matter Above the W Mass," Phys. Rev. D **41** (1990) 3565.

[35] E. W. Kolb and M. S. Turner, "The Early Universe," Front. Phys. **69** (1990) 1.

[36] P. Gondolo and G. Gelmini, "Cosmic abundances of stable particles: Improved analysis," Nucl. Phys. B **360** (1991) 145.

[37] M. Drees, M. M. Nojiri, "The Neutralino relic density in minimal $N = 1$ supergravity," Phys. Rev. **D47** (1993) 376-408 [arXiv:hep-ph/9207234].

[38] K. Griest, D. Seckel, "Three exceptions in the calculation of relic abundances," Phys. Rev. **D43** (1991) 3191-3203.

[39] J. R. Ellis, T. Falk and K. A. Olive, "Neutralino - Stau coannihilation and the cosmological upper limit on the mass of the lightest supersymmetric particle," Phys. Lett. B **444** (1998) 367 [arXiv:hep-ph/9810360]; J. R. Ellis, T. Falk, K. A. Olive and M. Srednicki, "Calculations of neutralino-stau coannihilation channels and the cosmologically relevant region

of MSSM parameter space," Astropart. Phys. **13** (2000) 181 [Erratum-ibid. **15** (2001) 413] [arXiv:hep-ph/9905481].

[40] M. Cirelli, R. Franceschini and A. Strumia, "Minimal Dark Matter predictions for galactic positrons, anti-protons, photons," Nucl. Phys. B **800** (2008) 204 [arXiv:0802.3378 [hep-ph]]; M. Cirelli, M. Kadastik, M. Raidal and A. Strumia, "Model-independent implications of the e+-, anti-proton cosmic ray spectra on properties of Dark Matter," Nucl. Phys. B **813** (2009) 1 [arXiv:0809.2409 [hep-ph]].

[41] O. Adriani *et al.* [PAMELA Collaboration], "An anomalous positron abundance in cosmic rays with energies 1.5-100 GeV," Nature **458** (2009) 607 [arXiv:0810.4995 [astro-ph]].

[42] S. W. Barwick *et al.* [HEAT Collaboration], "Measurements of the cosmic ray positron fraction from 1-GeV to 50-GeV," Astrophys. J. **482** (1997) L191 [arXiv:astro-ph/9703192].

[43] M. Aguilar *et al.* [AMS-01 Collaboration], "Cosmic-ray positron fraction measurement from 1 to 30-GeV with AMS-01," Phys. Lett. B **646** (2007) 145 [arXiv:astro-ph/0703154].

[44] M. Ackermann *et al.* [The Fermi LAT Collaboration], "Measurement of separate cosmic-ray electron and positron spectra with the Fermi Large Area Telescope," Phys. Rev. Lett. **108** (2012) 011103 [arXiv:1109.0521 [astro-ph.HE]].

[45] J. Hisano, S. Matsumoto and M. M. Nojiri, "Explosive dark matter annihilation," Phys. Rev. Lett. **92** (2004) 031303 [arXiv:hep-ph/0307216]; J. Hisano, S. Matsumoto, M. M. Nojiri and O. Saito, "Non-perturbative effect on dark matter annihilation and gamma ray signature from galactic center," Phys. Rev. D **71** (2005) 063528 [arXiv:hep-ph/0412403].

[46] M. Cirelli, A. Strumia and M. Tamburini, "Cosmology and Astrophysics of Minimal Dark Matter," Nucl. Phys. B **787** (2007) 152 [arXiv:0706.4071 [hep-ph]].

[47] N. Arkani-Hamed, D. P. Finkbeiner, T. R. Slatyer and N. Weiner, "A Theory of Dark Matter," Phys. Rev. D **79** (2009) 015014 [arXiv:0810.0713 [hep-ph]].

[48] D. Feldman, Z. Liu and P. Nath, "PAMELA Positron Excess as a Signal from the Hidden Sector," Phys. Rev. D **79** (2009) 063509 [arXiv:0810.5762 [hep-ph]].

[49] M. Ibe, H. Murayama and T. T. Yanagida, "Breit-Wigner Enhancement of Dark Matter Annihilation," Phys. Rev. D **79** (2009) 095009 [arXiv:0812.0072 [hep-ph]].

[50] W.-L. Guo and Y.-L. Wu, "Enhancement of Dark Matter Annihilation via Breit-Wigner Resonance," Phys. Rev. D **79** (2009) 055012 [arXiv:0901.1450 [hep-ph]].

[51] R. Barbieri, L. J. Hall and V. S. Rychkov, "Improved naturalness with a heavy Higgs: An alternative road to LHC physics," Phys. Rev. D **74** (2006) 015007 [arXiv:hep-ph/0603188].

[52] L. Lopez Honorez, E. Nezri, J. F. Oliver and M. H. G. Tytgat, "The Inert Doublet Model: An Archetype for Dark Matter," JCAP **0702** (2007) 028 [arXiv:hep-ph/0612275].

[53] E. M. Dolle and S. Su, "The Inert Dark Matter," Phys. Rev. D **80** (2009) 055012 [arXiv:0906.1609 [hep-ph]].

[54] J. Silk, K. A. Olive and M. Srednicki, "The Photino, the Sun and High-Energy Neutrinos," Phys. Rev. Lett. **55** (1985) 257.

[55] L. M. Krauss, M. Srednicki and F. Wilczek, "Solar System Constraints and Signatures for Dark Matter Candidates," Phys. Rev. D **33** (1986) 2079.

[56] K. Freese, "Can Scalar Neutrinos or Massive Dirac Neutrinos Be the Missing Mass?," Phys. Lett. B **167** (1986) 295.

[57] T. K. Gaisser, G. Steigman and S. Tilav, "Limits on Cold Dark Matter Candidates from Deep Underground Detectors," Phys. Rev. D **34** (1986) 2206.

[58] K. Griest and D. Seckel, "Cosmic Asymmetry, Neutrinos and the Sun," Nucl. Phys. B **283** (1987) 681 [Erratum-ibid. B **296** (1988) 1034].

[59] S. Ritz and D. Seckel, "Detailed Neutrino Spectra From Cold Dark Matter Annihilations In The Sun," Nucl. Phys. B **304** (1988) 877.

[60] M. Kamionkowski, "Energetic neutrinos from heavy neutralino annihilation in the sun," Phys. Rev. D **44** (1991) 3021.

[61] M. Kamionkowski, K. Griest, G. Jungman and B. Sadoulet, "Model independent comparison of direct versus indirect detection of supersymmetric dark matter," Phys. Rev. Lett. **74** (1995) 5174 [arXiv:hep-ph/9412213].

[62] H.-C. Cheng, J. L. Feng and K. T. Matchev, "Kaluza-Klein dark matter," Phys. Rev. Lett. **89** (2002) 211301 [arXiv:hep-ph/0207125].

[63] D. Hooper and G. D. Kribs, "Probing Kaluza-Klein dark matter with neutrino telescopes," Phys. Rev. D **67** (2003) 055003 [arXiv:hep-ph/0208261].

[64] E. Ma and M. Raidal, "Neutrino mass, muon anomalous magnetic moment, and lepton flavor nonconservation," Phys. Rev. Lett. **87** (2001) 011802 [Erratum-ibid. **87** (2001) 159901] [arXiv:hep-ph/0102255].

[65] K. Hayasaka, "Recent Tau Decay Results at B Factories -Lepton Flavor Violating Tau Decays," arXiv:1010.3746 [hep-ex].

[66] K. Nakamura *et al.* [Particle Data Group Collaboration], "Review of particle physics," J. Phys. G G **37** (2010) 075021 and 2011 partial update for the 2012 edition.

[67] E. Dolle, X. Miao, S. Su and B. Thomas, "Dilepton Signals in the Inert Doublet Model," Phys. Rev. D **81** (2010) 035003 [arXiv:0909.3094 [hep-ph]];

[68] M. Gustafsson, S. Rydbeck, L. Lopez-Honorez and E. Lundstrom, "Status of the Inert Doublet Model and the Role of multileptons at the LHC," arXiv:1206.6316 [hep-ph].

[69] M. Cirelli, N. Fornengo and A. Strumia, "Minimal dark matter," Nucl. Phys. B **753** (2006) 178 [arXiv:hep-ph/0512090].

[70] D. Schmidt, T. Schwetz and T. Toma, "Direct Detection of Leptophilic Dark Matter in a Model with Radiative Neutrino Masses," Phys. Rev. D **85** (2012) 073009 [arXiv:1201.0906 [hep-ph]].

[71] L. Lopez Honorez and C. E. Yaguna, "A new viable region of the inert doublet model," JCAP **1101** (2011) 002 [arXiv:1011.1411 [hep-ph]].

[72] J. R. Ellis, A. Ferstl and K. A. Olive, "Reevaluation of the elastic scattering of supersymmetric

dark matter," Phys. Lett. B **481** (2000) 304 [arXiv:hep-ph/0001005].

[73] E. Aprile *et al.* [XENON100 Collaboration], "Dark Matter Results from 100 Live Days of XENON100 Data," Phys. Rev. Lett. **107** (2011) 131302 [arXiv:1104.2549 [astro-ph.CO]].

[74] G. Angloher, M. Bauer, I. Bavykina, A. Bento, A. Brown, C. Bucci, C. Ciemniak and C. Coppi *et al.*, "Commissioning Run of the CRESST-II Dark Matter Search," arXiv:0809.1829 [astro-ph].

[75] V. N. Lebedenko, H. M. Araujo, E. J. Barnes, A. Bewick, R. Cashmore, V. Chepel, A. Currie and D. Davidge *et al.*, "Result from the First Science Run of the ZEPLIN-III Dark Matter Search Experiment," Phys. Rev. D **80** (2009) 052010 [arXiv:0812.1150 [astro-ph]].

[76] Z. Ahmed *et al.* [The CDMS-II Collaboration], "Dark Matter Search Results from the CDMS II Experiment," Science **327** (2010) 1619 [arXiv:0912.3592 [astro-ph.CO]].

[77] C. E. Aalseth *et al.* [CoGeNT Collaboration], "Results from a Search for Light-Mass Dark Matter with a P-type Point Contact Germanium Detector," Phys. Rev. Lett. **106** (2011) 131301 [arXiv:1002.4703 [astro-ph.CO]].

[78] R. Bernabei *et al.* [DAMA and LIBRA Collaborations], "New results from DAMA/LIBRA," Eur. Phys. J. C **67** (2010) 39 [arXiv:1002.1028 [astro-ph.GA]].

[79] S. C. Kim, H. Bhang, J. H. Choi, W. G. Kang, B. H. Kim, H. J. Kim, K. W. Kim and S. K. Kim *et al.*, "New Limits on Interactions between Weakly Interacting Massive Particles and Nucleons Obtained with CsI(Tl) Crystal Detectors," arXiv:1204.2646 [astro-ph.CO].

[80] T. Bruch [CDMS Collaboration], "CDMS-II to SuperCDMS: WIMP search at a zeptobarn," arXiv:1001.3037 [astro-ph.IM].

[81] M. Selvi [XENON1T Collaboration], "Study of the performances of the shield and muon veto of the XENON1T experiment," PoS IDM **2010** (2011) 053.

[82] H. Sekiya, "Xmass," J. Phys. Conf. Ser. **308** (2011) 012011 [arXiv:1006.1473 [astro-ph.IM]].

[83] F. Aharonian *et al.* [HESS Collaboration], "Very high-energy gamma rays from the direction of Sagittarius A*," Astron. Astrophys. **425** (2004) L13 [arXiv:astro-ph/0408145]; F. Aharonian *et al.* [H.E.S.S. Collaboration], "H.E.S.S. observations of the Galactic Center region and their possible dark matter interpretation," Phys. Rev. Lett. **97** (2006) 221102 [Erratum-ibid. **97** (2006) 249901] [arXiv:astro-ph/0610509].

[84] W. B. Atwood *et al.* [LAT Collaboration], "The Large Area Telescope on the Fermi Gamma-ray Space Telescope Mission," Astrophys. J. **697** (2009) 1071 [arXiv:0902.1089 [astro-ph.IM]].

[85] J. Aleksic *et al.* [MAGIC Collaboration], "MAGIC Gamma-Ray Telescope Observation of the Perseus Cluster of Galaxies: Implications for Cosmic Rays, Dark Matter and NGC 1275," Astrophys. J. **710** (2010) 634 [arXiv:0909.3267 [astro-ph.HE]].

[86] V. A. Acciari *et al.* [VERITAS Collaboration], "VERITAS Search for VHE Gamma-ray Emission from Dwarf Spheroidal Galaxies," Astrophys. J. **720** (2010) 1174 [arXiv:1006.5955 [astro-ph.CO]].

[87] M. Gustafsson, E. Lundstrom, L. Bergstrom and J. Edsjo, "Significant Gamma Lines from

Inert Higgs Dark Matter," Phys. Rev. Lett. **99** (2007) 041301 [arXiv:astro-ph/0703512].

[88] D. Suematsu, T. Toma and T. Yoshida, "Enhancement of the annihilation of dark matter in a radiative seesaw model," Phys. Rev. D **82** (2010) 013012 [arXiv:1002.3225 [hep-ph]].

[89] P. Agrawal, E. M. Dolle and C. A. Krenke, "Signals of Inert Doublet Dark Matter in Neutrino Telescopes," Phys. Rev. D **79** (2009) 015015 [arXiv:0811.1798 [hep-ph]].

[90] R. Abbasi *et al.* [IceCube Collaboration], "Multi-year search for dark matter annihilations in the Sun with the AMANDA-II and IceCube detectors," Phys. Rev. D **85** (2012) 042002 [arXiv:1112.1840 [astro-ph.HE]].

[91] T. Tanaka *et al.* [Super-Kamiokande Collaboration], "An Indirect Search for WIMPs in the Sun using 3109.6 days of upward-going muons in Super-Kamiokande," Astrophys. J. **742** (2011) 78 [arXiv:1108.3384 [astro-ph.HE]].

[92] J. D. Zornoza, "Dark matter search with the ANTARES neutrino telescope," arXiv:1204.5066 [astro-ph.HE].

[93] F. Halzen and S. R. Klein, "IceCube: An Instrument for Neutrino Astronomy," Rev. Sci. Instrum. **81** (2010) 081101 [arXiv:1007.1247 [astro-ph.HE]].

[94] P. Scott *et al.* [the IceCube Collaboration], "Use of event-level neutrino telescope data in global fits for theories of new physics," arXiv:1207.0810 [hep-ph].